Indian Journal of Engineering & Materials Sciences
Vol. 13, August 2006, pp. 339-346

Microstructural features, electrical and optical properties of nanostructured InSb thin films deposited at 373 K

Sukhvir Singh[a], A K Srivastava[a]*, K Lal[a], Y Tomokiyo[b], S K Sharma[a] & R Kishore[a]

[a]Electron Microscope Section, Division of Materials Characterization,

National Physical Laboratory, Dr K S Krishnan Road, New Delhi 110 012, India

[b]Research Laboratory for High Voltage Electron Microscopy, Kyushu University, Kasuga, Fukuoka 816-8580, Japan

Received 2 January 2006; accepted 17 May 2006

Thin films of InSb nanocrystals have been deposited onto KCl substrate using a thermal evaporation technique under high vacuum conditions (~10^{-6} torr). An intriguing microstructure consisted of moiré fringes with variable spacings and a corresponding variety of electron diffraction patterns in reciprocal space are reported at the deposition temperature of 373 K. The nanograins of InSb with preferred orientation and faceted morphology are delineated. A possible mechanism has been postulated to explain the evolution of such microstructures. It has been noticed that there is a peculiarity in the resistivity characteristics and infrared transmittance measurements obtained on these films. A set of electron micrographs, diffraction patterns and properties have been evaluated and discussed to understand the role of nanocrystals constituting the thin film, and certain types of defects introduced in the microstructure while deposition, on these properties.

IPC Code: H01C17/075

The preparation and characterization of thin films of compound semiconductors, especially of III-V group elements have gained importance in recent years as these materials have been proven technologically very useful for magnetic sensors, high speed electronic and galvanometric devices and infrared detectors in different wavelength ranges[1-3]. Some of the III-V compounds such as InSb, InP, AlSb, GaAs and GaSb have high electron mobility which makes them useful for many optoelectronic applications[4-7]. The electrical and optical properties of these semiconductors in bulk are widely investigated under various conditions of processing as well as annealing treatments to understand their performance[8-11]. Bulk InSb crystals are grown using different methods like Czocharalski[12], Bridgman[13-15], zone refining[16], vertical gradient[17] and centrifuge[18].

Thin films of InSb are applicable as Hall effect devices, magnetoresistance and tuning in infrared lasers and detectors[11,19,20]. These films have been finding significant applications in device fabrication, used as position detectors, direct drive motors or components of electronic equipments[21-25]. Extensive work has been devoted to improve the quality of InSb films prepared by liquid phase epitaxy[26], metal organic vapour phase epitaxy[27], molecular beam epitaxy[28,29] hot wall epitaxy[4] and sputtering[30]. In the past, several aspects of InSb thin films have been studied[31,32]. The structural and optical properties of narrow band gap semiconductors such as InSb, InP and InAs have been investigated[33]. X-ray diffraction and auger spectroscopy photoemission were used to study the interface and subsequent growth of InSb on Si (100)[34]. $In_{1-x}Sb_x$ films prepared by flash evaporation technique were characterized to correlate the microstructure with optical properties[35,36]. Relatively little work has been carried out on the structural investigations of thin films of InSb. In our previous reports a brief about the microstructural investigations on thin films of AlSb and InSb with stoichiometry prepared by thermal evaporation technique under high vacuum conditions has been discussed[37-39]. In AlSb thin film it was demonstrated that the change of process parameters play a very important role while deposition of a uniform thin film having a single phase of AlSb with cubic (fcc) lattice structure. A systematic study on the preparation and characterization of InSb thin films is under way to investigate the effect of parameters like nature of the substrates and deposition temperatures to optimize the conditions for the deposition of thin film with epitaxial in nature.

In the present investigations a detail study has been carried out to analyze the evolution of nanocrystals of

*For correspondence (E-mail: aks@mail.nplindia.ernet.in)

InSb thin film deposited on KCl substrate at the deposition temperature of 373 K. A novel microstructure of these films consisting of moiré fringes has been explained on the basis of postulating certain mechanisms that has presumably occurred while nucleation and growth during deposition. It has been studied that the defects introduced at the interfaces and grain boundaries of these tiny crystals may alter the electrical as well as optical properties of these films. A variety of electron diffraction patterns and microstructures have been observed and discussed to understand the anomalous properties noted in these films.

Experimental Procedure

Preparation of thin films

Synthesis of InSb compound has been carried out by vertical directional solidification (VDS) technique, using high purity indium (5N) and antimony (5N). The compound was grown in a conical quartz ampoule without using seed. The loss of antimony related problem was reduced by employing a closed quartz ampoule, which was sealed under high vacuum (10^{-6} torr). The quartz ampoule with ~0.015 m in diameter and 0.15 m in length has been heated in a resistive vertical muffle furnace which is fully temperature controlled. The compound was placed in a constant temperature zone of the furnace for melting. The temperature of the furnace was raised up to 1073 K and maintained for 4 h for synthesis and homogeneous mixing of the source material. For the growth of good quality crystals, the ampoule was lowered to the gradient-zone of the furnace at the rate of 0.005 mh^{-1} having temperature range of 848-923 K. Thin films of InSb are grown from the bulk compound using a thermal evaporation technique under high vacuum condition (10^{-6} torr) equipped with liquid N_2 trap.

In the present experiment a substrate of KCl has been used at 373 K to grow the film. These films are deposited to the thickness between 80 to 100 nm. Thin films are examined for elemental analysis and stoichiometry by an analytical transmission electron microscope make JEOL, model JEM 2000 FX. The transmission electron microscopes model JEM 200 CX and JEM 2000 FX operated at 200 kV have been used to investigate the microstructure of the films. The selected area electron diffraction patterns of the films are recorded for the determination of the crystallographic structure and orientation of the nanocrystallites constituting the thin film. X-ray diffractometry (XRD, model D8 Advance Bruker Axes) using CuK_α line was also utilized to analyze the crystal structure of InSb and if there is any preferred growth of nanocrystals. A scanning transmission electron microscope (STEM, VG-HB501) with a field emission gun, operated at 100 kV, has been employed to carry out the study of nano-sized grains, their size, shape, distribution and morphology.

Characterization

The infrared transmittance of the InSb thin films has been recorded using fourier transform infrared spectrophotometer (FTIR, Perkin and Elmer, system 2000 FT-IR) in the wave number range of 400-4000 cm^{-1}. InSb thin films have been deposited on to corning glass slides as substrate under same process conditions as mentioned above for the measurement of electrical resistivity with temperature varying from 300 to 473 K using Van der Pauw four probe technique in a vacuum of the order of 10^{-6} torr. The variation of electrical resistivity with temperature has been studied in detail for different deposition temperatures and band gap has been determined using the slope of the resistivity versus temperature curves. A curve has been plotted between the resistivity (σ) and 1000/*T*. Energy band gap was calculated from the slope of the resistivity versus temperature curve by using a simple equation of resistivity variation of the extrinsic semiconductor as a function of temperature.

Results and Discussion

Microstructural features induced during thermal evaporation

Thin films of InSb deposited at 373 K on KCl substrate have been examined using transmission electron microscopy techniques. These films are deposited to the thickness between 80-100 nm. Microstructural investigations delineated a set of fascinating nano-scaled features throughout the film. Figure 1a shows that fine grains are distributed randomly in the microstructure. In such polycrystalline structured films a large number of curly shaped grain boundaries are always expected and therefore the dislocations and other forms of lattice distortions in the matrix. The nanocrystallites of certain fraction having their planes orientation along the electron beam can be easily seen in Figs 1a and 1b. The microstructures depicted in Figs 1a and 1c reveals certain interesting features. It is seen that in addition to nanocrystallites observed in the microstructure, moiré fringes are clearly elucidated in the micrographs. These fringes originated in different

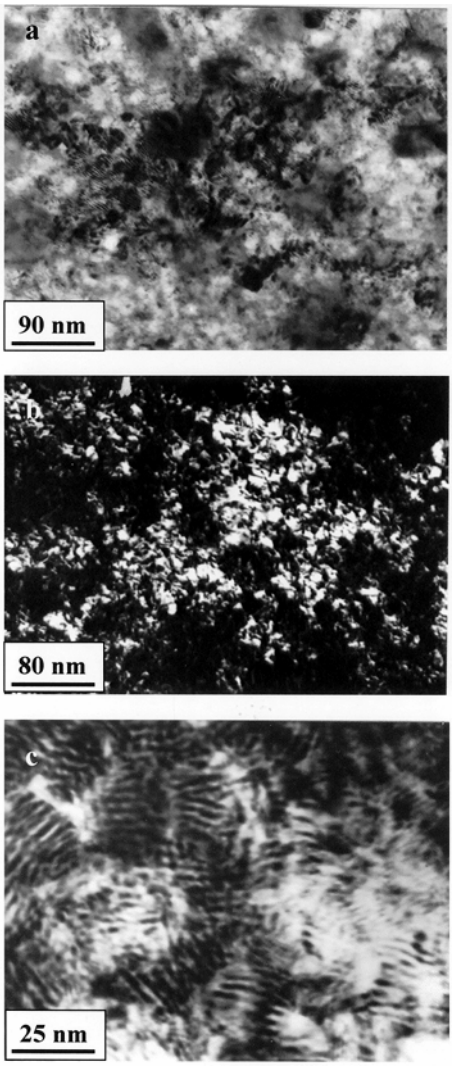

Fig. 1—TEM micrographs of the film showing (a) fine crystallites and an aggregate of moiré fringes, (b) size distribution of nanocrystallites and (c) high magnification image of moiré patterns of different fringe spacings

regions of the film also show different orientations with respect to other set of neighbouring fringes. A careful observation of these fringes depict orientation misfit characteristic. The moiré fringes in the micrograph has shown a set of varied spacings with a bending characteristic. It has been calculated from the micrograph (Fig. 1c) that the fringes have different spacings corresponding to 9, 19 and 28 Å (Figs 1a and 1c). It is known that in case of misfit fringes caused due to orientation differences, the fringe spacings are inversely proportional to misorientation of respective planes of two crystals. This mechanism clearly reflects that the misorientation between the fine grains overlapping each other in different regions is varied. During the process, since the deposition temperature

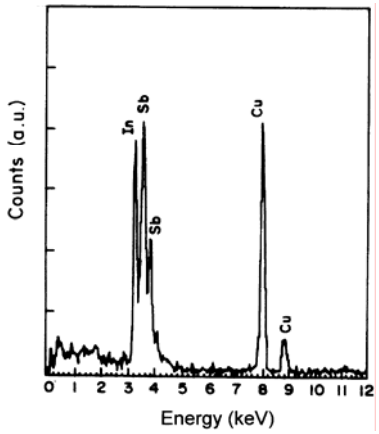

Fig. 2—Energy dispersive spectra recorded under TEM from the film deposited at 373 K, showing the peaks corresponding to In and Sb. Copper peaks are due Cu grid used to support the specimen.

(373 K) is not sufficient to satisfy the conditions for epitaxial growth, the rapid co-quenching of these elements on the substrate during deposition, may lead to strains at microscopic level. This would cause a lattice distortion and therefore defects in thin films. The bending feature of moiré fringes observed in the micrograph may be associated with a combined effect of strain phenomenon in lattice structure and orientation misfit between the crystals leading to rotational moiré fringes.

The compositional analysis of these films has been carried out using energy dispersive X-ray spectrometer attached with a transmission electron microscope. Thin films have been thoroughly scanned under the electron beam and it has been noticed that the stoichiometry of In and Sb in an equal proportion is uniform throughout the films deposited at different substrate temperatures of 300, 373 and 473 K. A typical EDS spectra recorded from a region of the film deposited at 373 K has been displayed as in Fig. 2. The peaks of In ($L_{\alpha 1}$) and Sb ($L_{\alpha 1}$, $L_{\beta 1}$) are clearly resolved in the energy range of 3-4.5 keV. The peaks corresponding to Cu ($K_{\alpha 2}$, K_{β}) in the energy range of 7.5-9 keV are due to the copper grid used as support for thin film under the TEM.

The selected area electron diffraction patterns recorded from various regions of thin films, elucidated the formation of single phase of cubic InSb (Fig. 3a). An interesting feature common in all these patterns is the streaks and diffused appearance of the spots in different reciprocal planes. An analysis of different rings show that they belong to the important planes of InSb cubic crystals, as marked on Fig. 3a. The lattice constant calculated from the electron

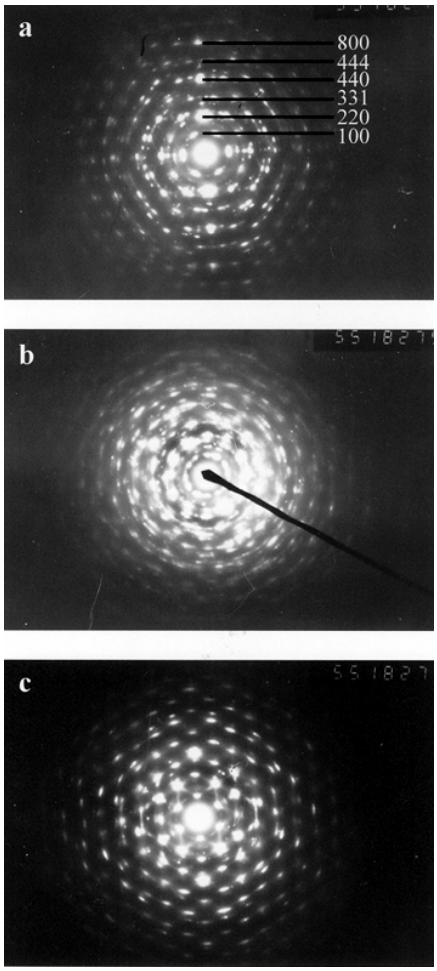

Fig. 3—A set of electron diffraction patterns (a, b & c) from different regions of the film showing the rings of various planes of cubic InSb and also the spots with streaks and distortions.

diffraction pattern; a = 0.65 nm, is found very close to that of standard lattice parameter of InSb cubic structure. The diffraction pattern in Fig. 3a further mimic that although the individual crystals in real space are misoriented with respect to each other but they have a common orientation along [111] zone axis of cubic lattice. Therefore, the individual spots are prominent along 3-fold on the ring pattern in reciprocal space. This phenomenon may also be considered as a texture generated during and after the nucleation of InSb crystals which tends to be epitaxial. Another feature of the presence of prominent streaks along with the spots in the electron diffraction pattern has been noticed (Fig. 3b and 3c). It has been well established that the streaks in the electron diffraction pattern may form due to lattice scale deviations in a crystal from a perfect structure. In the present investigations these deviations may be understood as distortions in terms of dislocations and

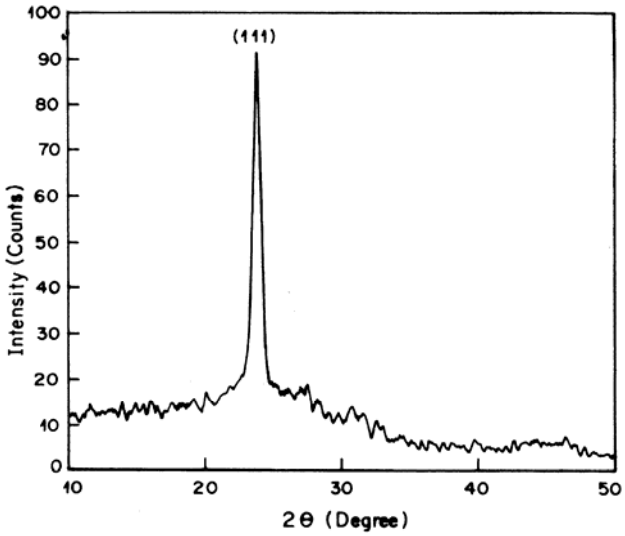

Fig. 4—An XRD pattern of thin film showing the peak corresponding to 111 planes of InSb cubic structure.

stacking faults. The diffraction patterns recorded from the microstructural features (Fig. 1) mimic the local semi-coherency during growth of InSb on KCl or aggregation of some grains with a small misorientation. The electron diffraction patterns (Fig. 3) suggests the possibility of grain growth lying along the electron beam direction, with a partial orientation with each other in the plane of the substrate. This phenomenon would reduce the number of rings in reciprocal plane due to the extinction condition applied for a cubic structure. However, a detailed study in this direction will be worthwhile. A prominent textured behaviour of thin films having a preferred orientation has also been delineated by XRD technique. It has been observed that there is only one strong peak along 111 planes of InSb cubic structure corresponding interplanar spacings, d = 0.374 nm (Fig. 4). It is important to mention that these films are deposited under similar conditions, several times to confirm the repeatability of the results. The evolution of microstructure in all set of experiments is same.

The investigations have been extended to characterize these films under high angle annular dark field imaging using a scanning transmission electron microscope. Figure 5 (a and b) exhibits the microstructures of the film delineating a distinct image of the grains in the specimen. The size distribution of the grains has been noticed quite uniform (~ less than 10-15 nm) with a clear facets in some of the individual grains. Figure 5b shows a faceted growth of an individual grain of about 15 nm in size, marked by a set of arrows. The striking

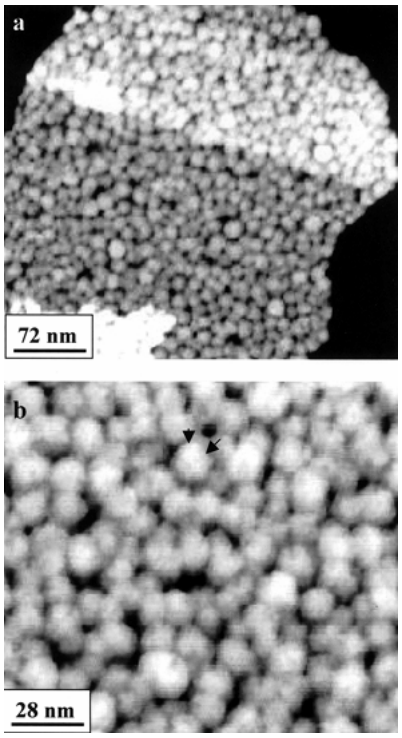

Fig. 5—STEM high angle annular dark field images of the film showing (a) fine and uniform distribution of nanosized grains and (b) faceted growth of the fine grains, a six facets grain-morphology is marked with an arrow.

feature viewed in the marked grain was the six facets surrounding it. The growth of six facets very well agrees with projected topography of a cubic crystal along one of the 3-fold axes. The selected area electron diffraction patterns (Fig. 3) also show a preferred 3-fold orientation of the planes projected on different rings in reciprocal space. The preferred orientation along 111 has also been elucidated by XRD (Fig. 4). This indicates that the resulting growth morphology of the InSb crystals preserve the symmetry of the cubic crystals. It is further seen that some of these grains are partially overlapped to each other which would cause the evolution of interference fringes, seen as moiré patterns in the bright field micrographs (Fig. 1).

Proposed explanation for the microstructures induced at 373 K

The microstructural features incited to explore the mechanism for the evolution of such unusual structural morphologies in these films. It is possible that after the primary nucleation at the substrate, the secondary nuclei in the vicinity of primary nuclei grow sufficiently large, such that a reasonable overlapping of these two crystals takes place. Since the temperature (373 K) is sufficiently low and the number of nuclei formed are large with constrained growth. A stage of rapid quenching during deposition results in a large fraction of fringes in the microstructure. It is well known that the large number of nuclei with constrained growth is always responsible for the fine grain microstructure. This phenomenon may not occur at 300 K, as the number of nuclei is large, however the growth is significantly constrained. If the growth of these nuclei were not even sufficient to have any intimate overlapping of grains in their vicinity, then the evolution of moiré fringes would not occur. In contrast, the deposition experiments at higher temperatures[14], e.g., 473 K and above are enough to provide sufficient mobility to the depositing atoms to have more systematic configuration during nucleation and growth process thereby avoiding the generation of moiré fringes.

It is important to discuss that such type of phenomenon may occur only if thermodynamic instability persists during the deposition. As mentioned above it is possible at low temperature, due to the constrained mobility of atoms, which experience a freezing tendency for a limited time during the deposition process. Under these circumstances, the energy associated with these structures will be higher, compared to the epitaxially grown films. This phenomenon also lead to the lattice strain and dislocation in the structure. Our observations are consistent with the presumed hypothesis of thermodynamic instability during deposition at 373 K. If the above explanation stands well at 373 K, then the unusual microstructure should also result at least at lower temperature, e.g., 300 K. However, the case is not so at lower temperature. It is possible that at lower temperature, the energy associated with the structures at microscopic level may not be able to provide suitable evolution of microstructure, as it is at 373 K.

It may be worthwhile to mention that if the deposition is carried out at a substrate temperature of 300 K the density of nucleation is expected to be high and the growth of the nuclei would continue as deposition proceeds. The adatoms at the temperature under consideration would condense at the point of strike causing simultaneous growth of the crystallites without any overlap. In contrast if the film is deposited at higher temperature (473 K) the density of nucleation is expected to be low and the mobility of the adatoms to be higher thereby the adatoms would be able to align themselves appropriately thus causing an increase of grain size. During the process of

growth of the film there would be no possibility of overlap of the grains. Thus in both the conditions the overlap of the crystallites would be avoided and it may not be possible to observe moiré fringes in the films deposited at 300 and 473 K.

A cross-sectional view of thin film deposited on KCl substrates at three different temperatures, 300, 373 and 473 K has been displayed as schematic in Fig. 6. It is suggested that the film grown at 300 K has finer details as compared to these films grown at 373 and 473 K. Coarsivity of the grain microstructure with the rising substrate temperature has been seen under the microscope. It has been postulated that the fine grains at 300 K deposition temperature are in true random orientation and therefore the electron diffraction pattern revealed the Debye rings. As the temperature of the substrate increases to 373 K, the deposition of InSb films leads to the growth of InSb cubic crystals in such a way that a large number of nuclei are formed and subsequently grown to a critical size. The overlapped crystals of the critical size in the microstructure may attain any random direction and therefore causes the formation of moiré fringes due to angular rotational difference of two sets of plane partially stacked over each other. It is surprising to note that this condition prevails to great extent when the thin films are synthesized at 373 K. A variety of electron diffraction patterns (Fig. 3) may also be explained on the basis of microstructure configured in Fig. 6. A plane view schematic simply exhibits that in reciprocal space the different crystallographic planes of InSb may originate Debye rings overlapped with spotty pattern. However, it also depends on the local variation of thin film at nano-scale that how the orientation of different planes are present and the boundaries in between are the centers of lattice scale defects leading to areas of strains in the film. As the temperature rises further the effect of rotational moiré fringes diminish and ultimately the deposition at high temperature leads to the formation of coarse grain microstructure.

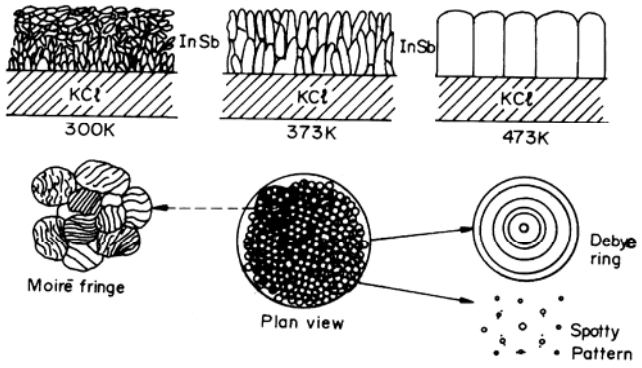

Fig. 6—A schematic showing cross-sectional view of the thin film deposited at 300, 373 and 473 K.

Electrical and optical measurements on thin films

The analysis of electrical resistivity and infrared transmittance of thermally evaporated thin films at 373 K has been presented and discussed. The data obtained has also been compared with the InSb thin films deposited at other temperatures to bring out the anomalies occur at the deposition temperature of 373 K.

The variation of electrical resistivity with temperature (300-473 K) of stoichiometric InSb thin film deposited at 373 K has been shown in Fig. 7a. For the comparison purpose, the variation of electrical resistivity with temperature of the film deposited at 300 and 473 K has also been plotted in Figs 7b and 7c. It has been seen that though the overall trend of the film deposited at 373 K was semiconducting in nature, as in case of the films deposited at 300 and 473 K, there are local fluctuations in resistivity measurements. It is important to mention that the resistivity measurements are conducted manually at different temperatures of the films under vacuum

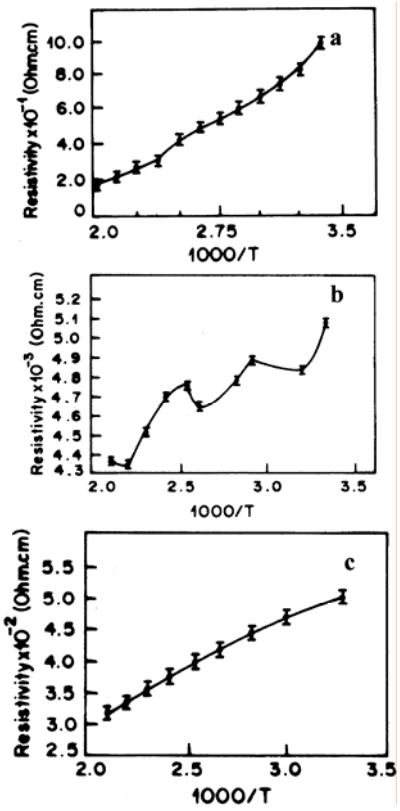

Fig. 7—Variation of resistivity with temperature of thin films deposited at (a) 300 K, (b) 373 K and (c) 473 K.

(better than 10^{-6} torr). These experiments were repeated many times to check the consistency of the data. There was no computer assisted phenomenon involved during measurements and therefore no noise or randomness in the resistivity data was anticipated. However, the minor variations realized in different readings (Fig. 7) have been indicated by putting error bars on each average value.

Figure 7 shows a set of important resistivity measurements, revealing a relationship between substrate temperature, grain size and resistivity. In general as the grain size increases, the resistivity should decrease. It is true if we compare the resistivity data of Fig. 7a (substrate temperature: 300 K) with Figs 7b and 7c (substrate temperatures: 373 and 473 K). However, the resistivity of the film deposited at 373 K (Fig. 7b) is noticed lower than the resistivity of the film deposited at 473 K (Fig. 7c). In the present investigation, this phenomenon can be explained on the basis of unusual microstructure of the film at 373 K containing normally a dense network of moiré fringes with varied spacings and defects, as reflected in Figs 1, 3 and 6. This unusual microstructure leads to a very fluctuating resistivity data at different temperatures (Fig. 7b) and it is difficult to imagine a true straight line-type data as depicted in Figs 7a and 7c. The energy band gaps obtained from the slopes of the resistivity versus temperatures have further indicated that there is a variation in the band gap (0.02-0.04 eV) calculated for the film deposited at 373 K in contrast to the stable band gaps of 0.11 and 0.05 eV obtained for the films deposited at 300 and 473 K, respectively.

The measurement of infrared transmittance using Fourier transform infrared spectrophotometer (FTIR) in the wave number range 400-4000 cm^{-1} carried on the InSb thin films deposited at 373 K has been compared with the films deposited at 300 and 473 K (Fig. 8). These spectra revealed that the transmittance increases with an increase of the temperature of deposition of thin film. The as deposited film at 373 K has nanocrystalline structure and has large number of grain boundaries, appeared as grain boundary phase. The grain boundary reflections result in more scattering of infrared radiation in the film. This scattered light has more chance to be absorbed by the film. Therefore a reduction in transmittance is observed for the as deposited film. However, as the temperature of deposition is increased to 473 K, only thermodynamically stable phases are present, in addition to the grain boundaries phases. This

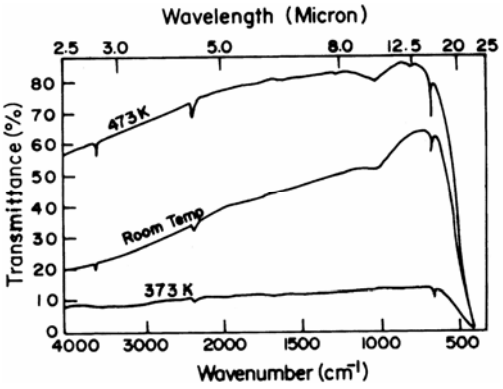

Fig. 8—Infrared transmission spectra of thin films deposited at 300, 373 and 473 K.

decreases in grain boundary areas in turn reduces the scattering of the infrared radiation in the film and results the increase in the transmittance. Optical energy band gap of thin film deposited at different temperatures has been calculated from the recorded IR transmittance spectra and found to be 0.08 eV which is comparable with the band gap calculated by the slope of the resistivity and temperature plot.

Conclusions

Nanostructured thin films of InSb have been deposited on KCl substrate at 373 K using a thermal evaporation technique. The microstructures and selected area electron diffraction patterns have exhibited the presence of unusual features of moiré fringes and lattice scale changes in cubic structure which are not seen in the film deposited at other temperatures under similar process conditions. A mechanism has been postulated to explain the fascinating microstructures that depend on the large number of nucleation sites followed by constrained growth. Subsequently the resistivity measurements and infrared transmittance of these films have been understood with microstructural features.

Acknowledgements

Dr. Vikram Kumar, Director, NPL is gratefully acknowledged for his encouragement. Dr. R. P. Pant is thanked to carry out the XRD measurements. One of the authors (AKS) thanks Professor C. Colliex (Orsay, France) for extending the facility of STEM, during the award of BOYSCAST fellowship by DST.

References

1 Isai M & Oshita M, *Rev Sci Instru,* 61 (1990) 1556.
2 Chen L P, Lou J J, Pang Y M & Yang S J, *Solid State Electron,* 35 (1992) 1081.

3 Chiang P K & Bedair M, *Appl Phys Lett*, 46 (1995) 383.
4 Singh T & Bedi R K, *Thin Solid Films*, 312 (1998) 111.
5 Raisin C L, Albert C, Birault B, Abdel F G & Voisin P, *Solid State Comm*, 61 (1987) 17.
6 Sharma S K, Tomokiyo Y, Singh S, Srivastava A K & Zaidi Z H, *J Mater Sci Lett*, 20 (2001) 2193.
7 Biefeld R M, Allerman A A & Kurtz S R, *J Cryst Growth*, 174 (1997) 593.
8 Senguttuvan M P, Moorthy B S & Ramasamy P, *J Cryst Growth*, 213 (2000) 51.
9 Wang Y, Regel L L & Wilcox R, *J Cryst Growth*, 209 (2000) 175.
10 Senguttuvan M P, Moorthy B S, Santhanaraghavan & Ramasamy P, *J Cryst Growth*, 200 (1999) 96.
11 Kroemer H, *Physica E*, 20 (2004) 196.
12 Lin M H & Kou S J, *J Cryst Growth*, 152 (1995) 256.
13 Mulski G & Neumann, *J Cryst Growth*, 59 (1982) 548.
14 Venkataraghavan R, Rao K S R K & Bhatt H L, *J Cryst Growth*, 186 (1998) 322.
15 Duffar T, Dusserre P, Picca F, Lacroix Giacometti N, *J Cryst Growth*, 211 (2000) 434.
16 Garamut J P, Differ T & Favier J J, *J Cryst Growth*, 106 (1990) 426
17 Jung Y J, Park M K, Tac S I, Lee K H & Lee J H, *J Appl Phys*, 69 (1991) 3109.
18 Zhou J L, Wilcox W R & Regel L L, *J Cryst Growth*, 128 (1993) 173.
19 Boch A J & Welzinis R G V, *J Appl Phys*, 58 (1985) 3434.
20 Welzinis R G V & Ridley B K, *Solid State Electron*, 27 (1984) 113.
21 Farrow R & Robertson D, Patent Application No. WO1981GB0000057 Date of publication 1981-10-01.
22 Kasai I & Toman J R, Patent Application No. US1994000252986 Date of publication 1997-07-08.
23 Lee S H, Patent Application No. US1997000918871 Date of publication 1999-01-19.
24 Berus T, Oszwaldowski M & Grabowski J, *Sensors Actuators A*: *Physical*, 116 75, 2004.
25 Szymonski M, Korecki P, Kolodziej J, Czukba P & Piatkowski P, *Thin Solid Films*, 367 (2000) 134.
26 Holunes D E & Kamath G S, *J Electron Mater*, 9 (1980) 95.
27 Chiang P K & Bedai S M, *Appl Phys Lett*, 46 (1995) 383.
28 Davis J L & Thomson P E, *Appl Phys Lett*, 54 (1989) 2235.
29 Zhang T, Clowes S K, Debnath M, Bennet A, Roberts A, Harris J J & Stradling R A & Cohen L F, *Appl Phys Lett*, 84 (2004) 4463.
30 Miyazaaki T, Kunugi M, Kitamure Y & Adachi S, *Thin Solid Films*, 287 (1996) 51.
31 Isai M, Yasuda S, Ogita M & Tanaka I, *J Appl Phys*, 71 (1992) 4567.
32 Goc J & Oszwaldowski M, *Thin Solid Films*, 116 (1984) 200.
33 Massida S, Contineza A, Freeman A J, Pascole T M D, Meloni F & Sena M, *Phys Rev B*, 41 (1990) 12079.
34 Franklin G E, Rich D H, Hong H, Miller T & Chian T C, *Phys Rev B*, 45 (1992) 3426.
35 Chou L H, *Thin Solid Films*, 215 (1992) 188.
36 Chou L H & Kuo M C, *J Appl Phys*, 77 (1995) 1964.
37 Lal K, Singh S, Kishore R, Sharma T P & Sharma S K, Indo – Japanese Symp. On Frontiers in Electron Microscopy in the 21st Century, Hyderabad, India, 1998.
38 Sharma S K, Tomokiyo Y & Singh S, *Annual Reports* HVEM LAB., Kyushu Univ. (Japan). 25 (2001) 3.
39 Lal K, Srivastava A K, Singh S & Kishore R, *J Mater Sci Lett*, 22 (2003) 515.